International Journal of Mathematics Trends and Technology
ISSN: 2231-5373/ https://doi.org/10.14445/22315373/IJMTT-V68I11P505
Volume 68 Issue 11, 46-62, November 2022

Modeling and Numerical Simulation of Incompressible Flows using a Pollutant Dispersion Approach

Aboubacar Sidiki Cisse, Roy Kiogora, Kennedy Awuor

[1] Mathematics Department Pan African University , Institute for Basic Science Technology and Innovation , kenya

[2] Mathematics Department Jomo Kenyatta University of Agriculture and Technology , Kenya

[3] Department of Mathematics and Acturial Science Kenyatta University (KU) Nairobi, Kenya.

Abstract

Pollution dispersion in water is of tremendous importance since it has a direct impact on water quality, particularly in the open ocean. Using experimental and computer tools, the behavior of contaminants spread in water has been anticipated. A mathematical model has been developed based on incompressible flow using a pollutants dispersion approach. These flows make up a substantial part of fluid mechanics and have applications in a variety of sectors, including aeronautics, machine propulsion, free flow hydraulics, and so on. We first established the general convection equation that control the flow of this type fluid, and then we performed several simulations of basic compressible flows of fluid mechanics, such as pollutant dispersion on the surface of a moving liquid. For the discretization of the terms occurring in the different equations of this model, the numerical resolution is based on the method of finite differences utilizing the Cranck Nicholson diagram and the analysis of the diffusion of pollutants, changeable position of the polluting source. We were able to establish data from the literature using the numerical method used in this investigation, displaying acceptable conformity.

Keywords: *Convection equation; finite difference method; dispersion of pollutants; fluid mechanics ; Cranck Nicholson.*

1 Introduction

Convective dispersion models are one of the most widely used models for assessing pollution transport and diffusion CHERCHEURS & DU TALENT (n.d.). They're simple to use, and the modeling is backed up by a lot of technological know-how. Convection-type dispersion models have progressed to a point of maturity (Campbell & Glass, 2000). As a result, they are now widely employed by authorities and numerous businesses as assessment tools. Draxler & Taylor (1982) developed a computer model based on real-time meteorological data to simulate the impact of wind shear on a single pollutant puff. The fact that these scale models may be used to predict pollution dispersion in unidirectional flows with reasonable confidence (such as those occurring on the surface of water). When the flows are stable and more challenging, they are less useful like for instance : Flows on abrasive surface, flows around obstacles and objects that are distinct terrain or flows wakes that are hypothetical situations. They confirmed the relation of puff spread to geostrophic wind speed under homogeneous conditions using Taylor's approach. With the remaining experimental data on long-range dispersion indicative of average circumstances, they determined that the findings of the method utilized and the computer simulation are both acceptable. Feng et al. (2021) Mechanical dispersion and physico-chemical dispersion are two different types of dispersion. The rate at which mechanical dispersion occurs is proportional to the flow velocity the phenomenon of dispersion is known as convection. Using a medium In porous flows, the average flow velocity is higher diffusion can happen in either the longitudinal or transverse flow directions. A physico-chemical dispersion is referred to as molecular diffusion. As a result, unlike mechanical dispersion, this phenomenon can also occur while the fluid is at rest(Milliez & Carissimo, 2007).

Environmental Impacts of Thermal and Brine Dispersion Using Hydrodynamic Modelling for Yanbu

Desalination Plant, on the Eastern Coast of the Red Se (Aljohani et al., 2022). The environmental implications of brine and thermal discharges from seawater desalination facilities near Yanbu, Saudi Arabia, on the Red Sea's southern shore, were the subject of this study. The calibrated three-dimensional numerical model Delft3d was used to investigate the effects of recirculation patterns and dispersions. The environmental impact assessment, identification, and characterization procedure might aid in the development of improved strategies for the planning and management of desalination-related technical solutions. When considering the presence of seasonal turbulent circulations, the magnitude of the flow near the position of the outflow was always large, according to the model simulations for the different seasons. The level of thermal and brine dispersion, as well as environmental compliance, were assessed. The well-mixed environment accelerated the process.

Numerical findings and stability of the ADI F. Wang et al. (2022) approach for two-dimensional advection-diffusion equations with a time step of half a second. They're interested in the stability and numerical results of the discretization for the two-dimensional advection-diffusion equation using the alternating implicit direct technique (ADI). The forward time difference and the central space difference are used to identify two-dimensional advection-diffusion. Then they obtained two matrices with the time step size and, in which this methodology is based on the ADI method. The Von-Neumann stability methodology is used to achieve stability, and the ADI method's stability feature is unconditionally stable (Nurwidiyanto & Ghani, 2022).

2 Mathematical Model

The development of the mathematical equations involved in the current study, as well as the definition of the equations that characterize the problem studied, the assumed hypothesis, and the therapeutic interventions of a pollutant on the surface of such an appears to move, is shown below. Deformable fluid flows are mathematically expressed using pollutant the effect of temporal variation in pollutant concentrations, mass conservation, and the independence of the z-quantity assumption. Physical and

mathematical foundations for these equations can be found in specialized literature. This study only considers incompressible flows. The following are the key assumptions:

i . The effect of temporal variation in pollutant quantity in an elementary volume (the Balance Equation)

$$\frac{c}{\partial t} = \nabla.(D\nabla c) - \nabla.(Vc) \tag{1}$$

where V denotes the quantity's velocity field , the gradient is represented by ∇ , reflects the divergence $\bigtriangledown.$, the concentration gradient is represented by ∇c in this equation.

ii . The fluid is Newtonian, and the flow is incompressible.

iii . The advection-diffusion equation with source term governs the transport of any scalar variable. The governing equations can be expressed in general terms using the assumptions mentioned above:

Mass conservation equation:

$$\frac{\partial c}{\partial t} + V.\nabla c = 0 \tag{2}$$

iv . Given the following assumptions about z's independence (neglecting variations along the vertical) and the diffusion coefficient D is constant :

$$\frac{\partial c}{\partial t} = \left(D\nabla^2 c - V\nabla c\right) = 0 \tag{3}$$

Using Cartesian coordinates, we get the following form:

$$\frac{\partial c}{\partial t} + V_1 \frac{\partial c}{\partial x} + V_2 \frac{\partial c}{\partial y} - D\left(\frac{\partial^2 c}{\partial x^2} + \frac{\partial^2 c}{\partial y^2}\right) = 0 \tag{4}$$

3 Order of magnitude analysis.

Problem (4) Bath et al. (2022) is a parabolic evolution problem with a convection term and a diffusion term, as is typical of fluid mechanics problems. We will first perform an order of magnitude analysis on each of these terms. Let φ be the order of magnitude of the various terms of equation (4) , and τ be the characteristic time: (Zhan et al., 2021)

$$\frac{\Delta c}{\tau} + V_1 \frac{\Delta c}{\varphi} + V_2 \frac{\Delta c}{\varphi} - D\left(\frac{\Delta c}{\varphi^2} + \frac{\Delta c}{\varphi^2}\right) = 0 \tag{5}$$

When only diffusion is taken into account, the typical time is:

$$\tau_d = \frac{\varphi^2}{D} \tag{6}$$

We calculate the characteristic time of diffusion W. Wang et al. (2022) for the heat equation. The time characteristic verifies a type of relationship (to be compared to the stability condition for a diffusion equation) .

$$\frac{D\tau_d}{\varphi^2} \approx 1 \tag{7}$$

It's the time it takes for diffusion phenomena Weerasekera et al. (2022) to decay exponentially.

If only convection is taken into account, the typical time is as follows:

$$\tau_c \approx \frac{\varphi}{V} \tag{8}$$

The time it takes for the spot to be transported by the velocity field over a distance equal to the task's dimension is referred to as this duration. As a result, the type relation is confirmed by this

characteristic time τ_c to be compared to the Ling et al. (2021) stability requirement of heat :

$$\frac{V\tau_c}{\varphi} \approx 1 \tag{9}$$

Another characteristic time of convection Faúndez-Zanuy (2022) can be defined for our problem: the time to leave τ_s outside the domain of the pollutant ω. It confirms the following using the domain's characteristic dimension K:

$$\frac{V\tau_s}{K} \approx 1 \tag{10}$$

Finally, the Péclet (P_e) number is the ratio of the characteristic periods of τ_d diffusion and τ_c convection:

$$\frac{\tau_d}{\tau_c} = \frac{V\varphi}{D} = P_e \tag{11}$$

which characterizes the relative importance of the convection term compared to the diffusion term. (Shamshuddin et al., 2022)

3.1 Convection diffusion of a Gaussian

The power to which e in the Gaussian function is raised in two dimensions is any negatively definite quadratic form. As a result, the Gaussian's level sets will always be ellipses (Szarek et al., 2022). Consider the following starting point: **?**

$$\Phi(x,y) = e^{-}\left(\frac{x-x_0}{r_0}\right)^2 e^{-}\left(\frac{y-y_0}{r_0}\right)^2 \tag{12}$$

This denotes a Gaussian spot with amplitude 1 and radius r_0 centered in (x_0, y_0). If no convection exists, this spot diffuses in a self-similar manner, i.e., its amplitude reduces and its radius grows while preserving a Gaussian Kopyev et al. (2022) form:

$$c(x,y,t) = A(t)e^{-}\left(\frac{x-x_0}{r_t}\right)^2 e^{-}\left(\frac{y-y_0}{r_t}\right)^2 \tag{13}$$

Rinaldi et al. (2022) Using the domain-wide global conservation of c:

$$\iint c(x,y,t)dxdy = \iint \Phi(x,y)dxdy = constant \tag{14}$$

The diffusion solution of equation (4) is therefore written:

$$c\,(x,y,t) = \left(\frac{r_0}{\sqrt{4Dt+r_0^2}}\right)^2 e^{-}\left(\frac{x-x_0}{\sqrt{4Dt+r_0^2}}\right)^2 e^{-}\left(\frac{y-y_0}{\sqrt{4kt+r_0^2}}\right)^2 \tag{15}$$

The amplitude of this Gaussian therefore decreases according to the law:

$$A(t) = \left(\frac{r_0}{\sqrt{4Dt+r_0^2}}\right)^2 \tag{16}$$

This Gaussian point is carried without deformation and diffuses along the velocity field's trajectories, as before, assuming convection by a velocity field without shear is taken into account. The trajectories are straight lines in a constant-speed field: (Chen et al., 2022)

$$x(t) = x_0 + v_1 t_1, y(t) = y_0 + v_2 t \tag{17}$$

The convection-diffusion solution of equation (4) is therefore written:

$$c(x,y,t) = \left(\frac{r_0}{\sqrt{4Dt+r^2}}\right)^2 e^{-}\left(\frac{x-x_0-v_1 t}{\sqrt{4Dt+r_0^2}}\right)^2 e^{-}\left(\frac{y-y_0-v_2 t}{\sqrt{4Dt+r_0^2}}\right)^2 \tag{18}$$

This is a solution in an infinite medium that does not consider the problem's boundary conditions (4). If the diameter of the spot r_0 is modest compared to the dimension K of the domain ω, it is a good estimate of the answer (Aghili, 2021) .

3.2 Diffusion eigenmodes

To seek solutions checking the boundary conditions, one determines first of all the eigen modes of diffusion Solders et al. (2022) using the variable separation method described in the analytical paragraph (Kubota & Piccinini, 2022) . The calculation is the same, and it is easily shown that the eigenmodes are the following functions:

The general diffusion solution is then a linear combination of its modes (Faúndez-Zanuy, 2022):

$$c(x,y,t) = \sum_{p=0}^{\infty}\sum_{q=0}^{\infty} \alpha_{p,q} c_{p,q}(x,y,t) \tag{19}$$

4 Method of solution

4.1 Finite difference method

The finite difference technique was used to solve the governing equations above. The final set of equations in finite difference form is given below. Liang et al. (2022). The Cranck Nicholson scheme Ngondiep (2022) is used to precisely discretize the parabolic problem (4) .

$$\frac{\partial c}{\partial t} + V_1 \frac{\partial c}{\partial x} + V_2 \frac{\partial c}{\partial y} - D\left(\frac{\partial^2 c}{\partial x^2} + \frac{\partial^2 c}{\partial y^2}\right) = 0 \tag{20}$$

$$\frac{c_{i,j}^{n+1} - c_{i,j}^{n}}{dt} = \frac{D}{dx^2}\left(c_{i+1,j}^{n} - 2c_{i,j}^{n} + c_{i-1,j}^{n}\right) + \frac{D}{dy^2}\left(c_{i,j+1}^{n} - 2c_{i,j}^{n} + c_{i,j-1}^{n}\right) - \frac{V_1}{dx}\left(c_{i+1,j}^{n} - c_{i,j}^{n}\right) - \frac{V_2}{dy}\left(c_{i,j+1}^{n} - c_{i,j}^{n}\right) \tag{21}$$

4.2 Method of implicit alternating directions(ADI)

.

The ADI methods work on the basis of decomposing spatial operators along the x and y directions of space (Ou et al., 2022) .

Equation (4) is written in the following symbolic form:

$$\frac{c_{i,j}^{*} - c_{i,j}^{n}}{dt/2} = -V_1 \frac{c_{i+1,j}^{*} - c_{i-1,j}^{*}}{2dx} + D\frac{u_{i+1,j}^{*} - 2c*_{i,j} + c_{i-1,j}^{*}}{dx^2} \tag{22}$$

$$-V_2 \frac{c_{i+1,j}^{n} - c_{i-1,j}^{n}}{2dx} + D\frac{c_{i+1,j}^{n} - 2c_{i,j}^{n} + c_{i-1,j}^{n}}{dx^2}$$

$$\frac{c_{i,j}^{n+1}-c_{i,j}^{*}}{dt/2}=-V_1\frac{c_{i+1,j}^{*}-c_{i-1,j}^{*}}{2dx}+D\frac{c_{i+1,j}^{*}-2c_{i,j}^{*}+c_{i-1,j}^{*}}{dx^2}$$

$$-V_2\frac{c_{i+1,j}^{n+1}-c_{i-1,j}^{n+1}}{2dx}+D\frac{c_{i+1,j}^{n+1}-2c_{i,j}^{n+1}+c_{i-1,j}^{n+1}}{dx^2} \tag{23}$$

Equation (21) can be written as Ax=b, where c^1 is the tridiagonal matrix and $c^1(c_{i,j}^n)$ is a vector along the N_x direction.

$$\begin{bmatrix} \dots & \dots & 0 & \dots & 0 \\ \ddots & \ddots & \ddots & \ddots & \vdots \\ 0 & a_1^1 & a_2^1 & a_3^1 & 0 \\ \vdots & \ddots & \ddots & \ddots & \ddots \\ 0 & \dots & 0 & \ddots & \ddots \end{bmatrix} \times \begin{bmatrix} \vdots \\ c_{i,j-1}^n \\ c_{i,j}^n \\ c_{i,j+1}^n \\ \vdots \end{bmatrix}$$

Equation (22) can be written along the N_y direction.

$$\begin{bmatrix} \dots & \dots & 0 & \dots & 0 \\ \ddots & \ddots & \ddots & \ddots & \vdots \\ 0 & a_1^1 & a_2^1 & a_3^1 & 0 \\ \vdots & \ddots & \ddots & \ddots & \ddots \\ 0 & \dots & 0 & \ddots & \ddots \end{bmatrix} \times \begin{bmatrix} \vdots \\ c_{i-1,j}^* \\ c_{i,j}^* \\ c_{i+1,j}^* \\ \vdots \end{bmatrix}$$

5 Results and Discussion

5.1 Diffusion eigenmode

we plot our amplitude by taking into account the p =1.5 and q = 1.5 with a coefficient k = 0.01 and a length L= 1m. The last time was taken to be Tf = 0.5. We observed that the amplitude of this diffusion is reducing; it declines with a value of 0.75 in the direction of the ordinates' axis.

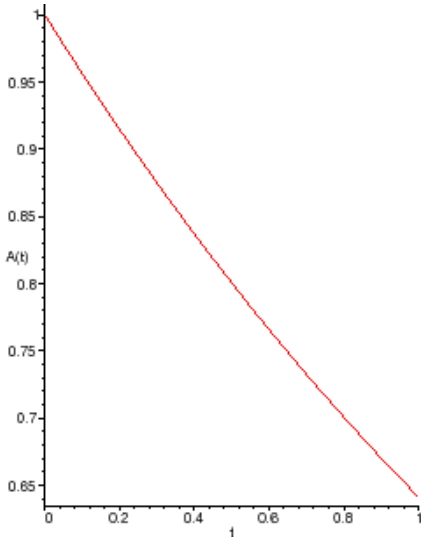

Figure 1: Mod of Amplitude

5.2 The solution's temporal evolution

With a mesh of Nx = Ny = 30 points in each direction and a parameter K= 0,01, we first simulate the diffusion of the correct mode in Fig. 4.1 to test the validity of this program. The solution estimated at time Tf = 0.5 with dt = 0.1 is presented; the shape of this solution matches the exact solution eigenmode of diffusion in Figure 4.1, which depicts the solution's temporal evolution at the point where x equals 1 and y equals 1.

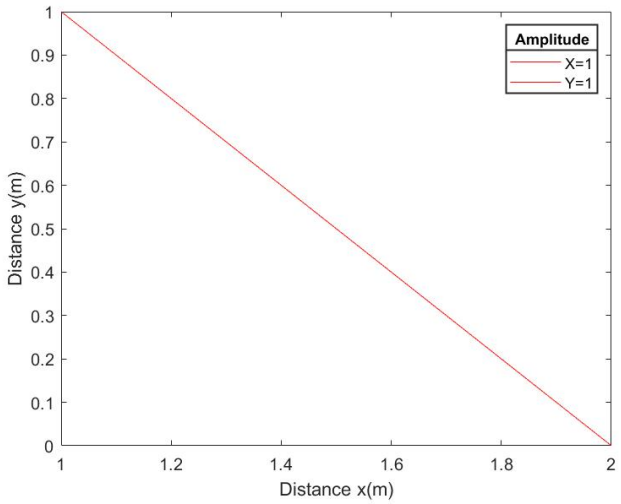

Figure 2: Diffusion eigenmode 001

5.3 solution for broadcasting using the ADI system

We calculated the inaccuracy at the location $x = 1$ and $y = 1$ at time 2 of the order of the typical diffusion time as a function of the integration step in time dt in order to understand the accuracy of the integration in time of the graphic. The trace of fig. 4.2 demonstrates that the error, for the selected time steps, is almost independent of the time step dt and is mostly a spatial discretization mistake. Keep in mind that the time steps chosen are substantially shorter than the typical diffusion time $dt << \tau_d \backsimeq 2.5$.

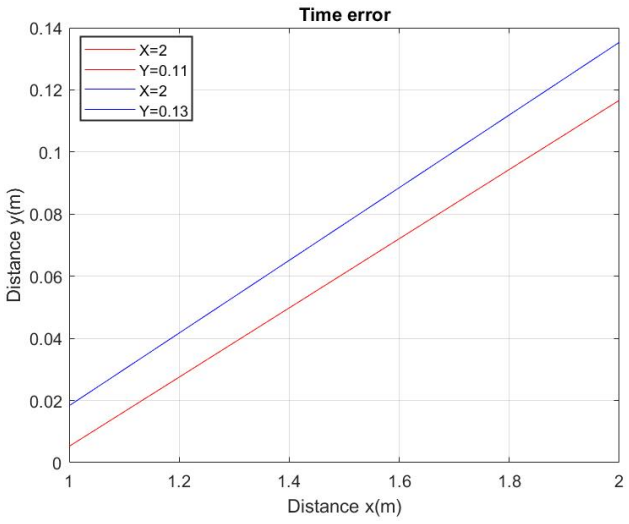

Figure 3: broadcast solution with the ADI scheme

5.4 Iso value of solution (during convection diffusion)

Note the convection that the initial solution does not deform, that is, it does not change the initial value. This indicates that boundary conditions allow the structure to leave the field. We also investigated the time evolution of the maximum value of the exact diffusion solution and the maximum value of the calculated solution. This hypothesis has shown that the disintegration of the solution is a viscous disintegration.

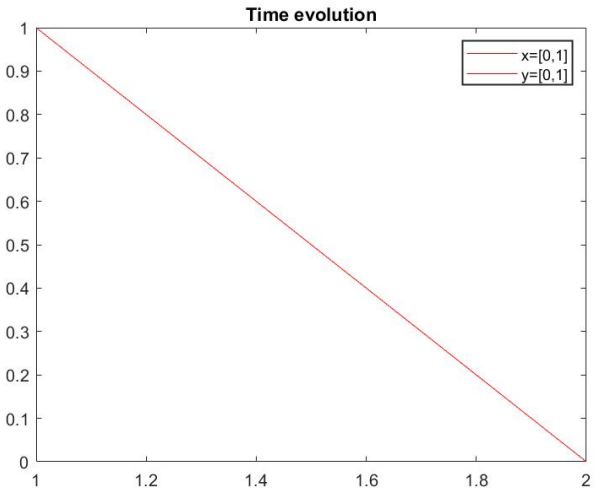

Figure 4: Iso value of solution

5.5 Numeric error in ADI schema

Next, Figure (4.6) shows the effect of the time dt integration step by plotting the difference between the maximum value of the exact diffusion solution and the maximum value of the calculated solution as a function of dt. It can be seen that this difference increases rapidly above the value $dt = 0.01$. This value is exactly in the range of characteristic convection time $\tau_c = 0.02$. To conclude this simulation, note that the choice of numerical parameters was determined by physics. It is a problem, not due to numerical stability constraints.

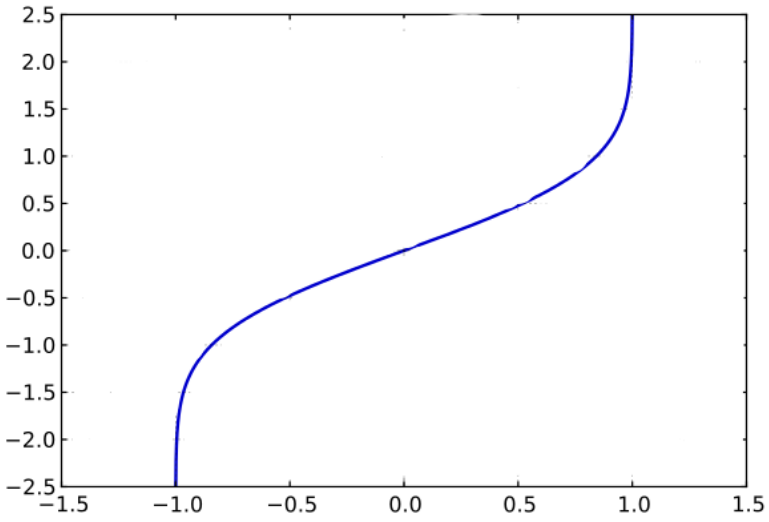

Figure 5: dt function error convection

5.6 Convection of a Gaussian:

Next, draw a convection and diffusion diagram of a Gaussian distribution with a diffusion constant $D = 10e-40m^2/s$ and a fluid velocity of 5 mm / s. The numerical solution is displayed in the initialized state after 1 millisecond. For mesh, $N_x = N_y = 30$ and time step $dt = 0.01$. The resolution was $t = 0.6$ seconds and $t = 0.7$ seconds.

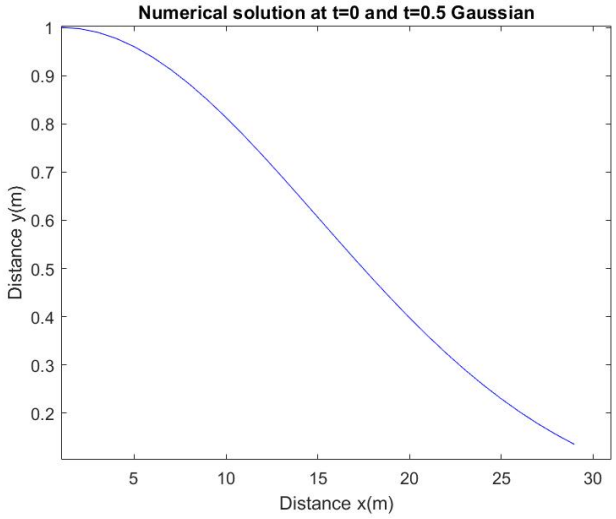

Figure 6: Convection of a Gaussian Numerical

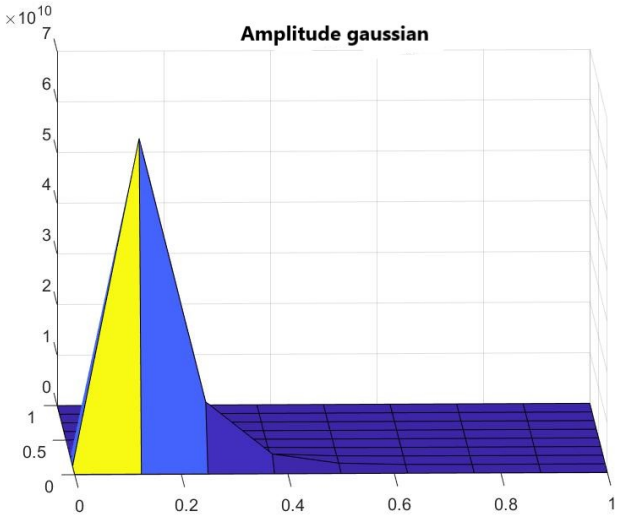

Figure 7: Convection of a Gaussian Numerical with amplitude

6 Conclusion

In this study, we proposed a finite difference method to find the exact solution of a system of ordinary differential equations resulting from the discretization of convection-diffusion equations for spatial variables. The discretion of many PDEs leads to this type of system, and the proposed method can be applied to calculate the exact solution of the system.

References

Aghili, A. (2021). Complete solution for the time fractional diffusion problem with mixed boundary conditions by operational method. *Applied Mathematics and Nonlinear Sciences*, *6*(1), 9–20.

Aljohani, N. S., Kavil, Y. N., Shanas, P. R., Al-Farawati, R. K., Shabbaj, I. I., Aljohani, N. H., … Abdel Salam, M. (2022). Environmental Impacts of Thermal and Brine Dispersion Using Hydrodynamic Modelling for Yanbu Desalination Plant, on the Eastern Coast of the Red Sea. *Sustainability*, *14*(8), 4389.

Bath, P. E., Gaitonde, A., & Jones, D. (2022). Reduced Order Aerodynamics and Flight Mechanics Coupling For Tiltrotor Aircraft Stability Analysis. In *Aiaa scitech 2022 forum* (p. 0284).

Campbell, A., & Glass, K. C. (2000). The legal status of clinical and ethics policies, codes, and guidelines in medical practice and research. *McGill LJ*, *46*, 473.

Chen, D., Liu, X., He, W., Xia, C., Gong, F., Li, X., & Cao, X. (2022). Effect of attenuation on amplitude distribution and b value in rock acoustic emission tests. *Geophysical Journal International*, *229*(2), 933–947.

CHERCHEURS, N. J., & DU TALENT, O. (n.d.). Recherche hepl.

Draxler, R. R., & Taylor, A. D. (1982). Horizontal dispersion parameters for long-range transport modeling. *Journal of Applied Meteorology and Climatology*, *21*(3), 367–372.

Faúndez-Zanuy, M. (2022). Speaker recognition by means of a combination of linear and nonlinear predictive models. *arXiv preprint arXiv:2203.03190*.

Feng, P., Kong, Y., Liu, M., Peng, S., & Shuai, C. (2021). Dispersion strategies for low-dimensional nanomaterials and their application in biopolymer implants. *Materials Today Nano*, *15*, 100127.

Kopyev, A. V., Kiselev, A. M., Il'yn, A. S., Sirota, V. A., & Zybin, K. P. (2022). Non-GaussianGeneralization of the Kazantsev–Kraichnan Model for a Turbulent Dynamo. *The Astrophysical Journal*, *927*(2), 172.

Kubota, L., & Piccinini, R. (2022). Eigenmode Decomposition of the Diffusion Equation: Applications to Pressure-Rate Deconvolution and Reservoir Pore Volume Estimation. *SPE Journal*, 1–19.

Liang, X., Peng, J., Zhang, X., Guo, J., & Zhang, Y. (2022). Analysis of the rcf crack detection phenomenon based on induction thermography. *Applied Optics*, *61*(16), 4809–4816.

Ling, Y., Li, Q., Zheng, H., Omran, M., Gao, L., Chen, J., & Chen, G. (2021). Optimisation on the stability of CaO-doped partially stabilised zirconia by microwave heating. *Ceramics International*, *47*(6), 8067–8074.

Milliez, M., & Carissimo, B. (2007). Numerical simulations of pollutant dispersion in an idealized urban area, for different meteorological conditions. *Boundary-Layer Meteorology*, *122*(2), 321–342.

Ngondiep, E. (2022). Unconditional stability over long time intervals of a two-level coupled MacCormack/Crank–Nicolson method for evolutionary mixed Stokes-Darcy model. *Journal of Computational and Applied Mathematics*, *409*, 114148.

Nurwidiyanto, N., & Ghani, M. (2022). Numerical results and stability of adi method to two-dimensional advection-diffusion equations with half step of time. In *Prisma, prosiding seminar nasional matematika* (Vol. 5, pp. 773–780).

Ou, C., Cen, D., Vong, S., & Wang, Z. (2022). Mathematical analysis and numerical methods for Caputo-Hadamard fractional diffusion-wave equations. *Applied Numerical Mathematics*, *177*, 34–57.

Rinaldi, E., Han, X., Hassan, M., Feng, Y., Nori, F., McGuigan, M., & Hanada, M. (2022). Matrix-model simulations using quantum computing, deep learning, and lattice monte carlo. *PRX Quantum*, *3*(1), 010324.

Shamshuddin, M. D., Mabood, F., Khan, W. A., & Rajput, G. R. (2022). Exploration of thermal Péclet number, vortex viscosity, and Reynolds number on two-dimensional flow of micropolar fluid through a channel due to mixed convection. *Heat Transfer*.

Solders, S. K., Galinsky, V. L., Clark, A. L., Sorg, S. F., Weigand, A. J., Bondi, M. W., & Frank, L. R. (2022). Diffusion mri tractography of the locus coeruleus-transentorhinal cortex connections using go-esp. *Magnetic Resonance in Medicine*, *87*(4), 1816–1831.

Szarek, D., Maraj-Zygmat, K., Sikora, G., Krapf, D., & Wyłomańska, A. (2022). Statistical test for anomalous diffusion based on empirical anomaly measure for gaussian processes. *Computational Statistics & Data Analysis*, *168*, 107401.

Wang, F., Khan, M. N., Ahmad, I., Ahmad, H., Abu-Zinadah, H., & Chu, Y.-M. (2022). Numerical solution of traveling waves in chemical kinetics: time-fractional fishers equations. *Fractals*, *30*(02), 2240051.

Wang, W., Cherstvy, A. G., Metzler, R., & Sokolov, I. M. (2022). Restoring ergodicity of stochastically reset anomalous-diffusion processes. *Physical Review Research*, *4*(1), 013161.

Weerasekera, N., Cao, S., & Shingdon, D. R. (2022). Phase Field Modeling of Ghost Diffusion in Sn-Ag-Cu Solder Joints. *European Journal of Applied Physics*, *4*(2), 28–34.

Zhan, H., Dong, W., Chen, S., Hu, D., Zhou, H., & Luo, J. (2021). Improved test method for convection heat transfer characteristics of carbonate fractures after acidizing etching. *Advances in Geo-Energy Research*, *5*(4), 376.